

Universal two-state reorientational dynamics of diatomic hydrides in fcc salt crystals

C. E. Mungan,* R. Lai, and A. J. Sievers

Laboratory of Atomic and Solid State Physics and Materials Science Center, Cornell University, Ithaca, New York 14853-2501

(Received 8 November 1995; revised manuscript received 24 April 1996)

The reorientational spectra in the mid- and far infrared of OH^- , OD^- , SH^- , SD^- , SeH^- , and TeH^- in a variety of different alkali halides are studied. All of these systems have $\sim 300\text{ cm}^{-1}$ modes due to librations of the diatomics about their centers of mass. A surprising change in the dynamics of these librational modes with increasing temperature is discovered: their absorption strengths are observed to disappear by $\sim 150\text{ K}$ in the sodium-chloride-structure hosts and reappear in the millimeter-wave region in the forms of generalized-Debye spectra. This is in striking contrast to what is expected on the basis of the estimated orientational barrier heights using the known librational frequencies. It also contrasts with the cesium-chloride-structure salts, where the librational strengths of the molecules are conserved up to RT. The temperature-dependent variations of the fcc systems can be explained using a thermally activated jump-rotational-diffusion model wherein each defect hops with temperature-dependent dwell times between two distinct elastic configurations of the lattice-defect system: one involving librational and the second supporting diffusive rotational states. [S0163-1829(96)00938-1]

I. INTRODUCTION

Until recently, the vibrational and orientational modes of the chalcogen hydrides, XH^- where $X=\{\text{O}, \text{S}, \text{Se}, \text{or Te}\}$, doped in alkali halides were believed to be well understood.¹⁻⁴ However, new experiments have uncovered two completely unexpected features of the dynamics of these systems.

First, measurements of the vibrational relaxation of the fundamental stretching modes of these diatomics^{5,6} indicate that their T_1 decay times are approximately 10^{-9} s, about seven orders of magnitude smaller than the relaxation times of CN^- in the same hosts.⁷ This discovery is very surprising because there exist no low-order nonradiative decay channels which can give rise to such rapid relaxation. In seeking to understand this phenomena, we have been led to consider a key difference between the dynamics of CN^- and XH^- , namely the nature of their orientational modes. While CN^- exhibits marked P and R branches due to quasifree rotations and only manifests librational motion at very low energies (and hence temperatures),^{8,9} XH^- has a much lower moment of inertia, leading to high-frequency librations and to a lack of distinct rotational sidebands.^{2,10,11}

Secondly, it has been observed that the absorption strength of the fundamental librational mode of XH_2 in various fcc crystals is strongly temperature dependent.^{6,12} Yet at the same time, the center frequency and width of the infrared (IR) peak is not found to vary significantly, indicating that the orientational potential is not thermally softened. The discovery that the oscillator strength lost by the librations reappears in the millimeter-wave region as a Debye diffusional spectrum led us to propose that the XH^- defects are able to access two distinct elastic configurations: a low-temperature harmonic state and a higher-energy rotational well separated from the harmonic configuration by a large potential barrier. The existence of two, rather than only one, local configurations of the systems may open up multiple new pathways for vibrational relaxation. In order to investigate this possibility,

a more complete investigation of the experimental and theoretical nature of the orientational potential is called for.

In the present paper, IR measurements of the orientational modes of six different diatomics (OH^- , OD^- , SH^- , SD^- , SeH^- , and TeH^-) doped in various salt crystals are reported. In combination with the stretching vibrations of these molecular ions, librational sideband modes are observed at frequencies of $\sim 300\text{ cm}^{-1}$. The absorption strengths of these modes are found to vanish in the sodium-chloride-structure hosts by $\sim 150\text{ K}$. In their place, a Debye-like spectrum appears in the very far infrared. We are able to explain this phenomenon by using a two-elastic-configuration jump-rotational-diffusion model,¹² which we generalize here from 1 to 2 degrees of angular freedom. This identification of two distinct elastic configurations for the defect-lattice system implies that the dynamics of these simple molecules are richer than has previously been believed. Specifically, they simultaneously exhibit librational motion characteristic of the Devonshire potential for perfect crystals, diffusive rotations traditionally attributed to the Debye model of liquids, and a hopping behavior which is usually associated with glasses.

The organization of the paper is as follows. Section II A briefly summarizes the important experimental details and Sec. II B then presents careful measurements of the librational modes of the impurities, both as vibrational sidebands and directly in the far-infrared (FIR). Emphasis is placed upon deducing the unusual temperature dependences of these modes. The third subsection concerns very-far-infrared measurements of a representative SH^- sample, which indicate that the absorption strength lost by the librational modes is compensated for by the growth of a generalized-Debye spectrum. Section III is devoted to a discussion of the thermal behavior of the defect in terms of a model wherein the molecule librates in one low-energy elastic configuration, while in a second higher-energy configuration it rotationally diffuses, so that with increasing temperature the absorption strength associated with the high-frequency librational mode

is transferred to a low-frequency Debye-like spectrum.

II. EXPERIMENTAL MEASUREMENTS

A. Experimental details

Single crystals of XH^- doped in various alkali halides were grown by the Czochralski technique in an inert or reducing atmosphere at Cornell University and at the University of Illinois. For the sideband measurements the impurity concentrations were as large as possible, up to nominally ~ 0.5 mol % (at or near the observed solubility limits), in order to resolve the weak reorientational modes.

Infrared-absorption spectra in the vibrational sideband and direct librational frequency region were collected using a Fourier-transform interferometer, at either 1 or 4 cm^{-1} resolution. Samples were cooled to temperatures as low as 1.7 K using an optical-access liquid-helium cryostat. For a given sample, the sideband spectra were collected as rapidly as possible for a sequence of temperatures with a fixed sample placement and interferometer setup, in order to minimize variations in the backgrounds of the spectra. Such variations can include small changes in the baseline due to varying optical paths through or surface qualities of the sample if it is displaced in any way, and due to absorption by species such as residual atmospheric CO_2 or mechanical pump oil on the evacuated optics, which slowly vary with time.

Millimeter-wave absorption measurements in the 2–20 cm^{-1} frequency range were performed for two different SH^- crystals using a lamellar interferometer and a liquid- ^3He cryostat equipped with a light pipe. These spectra were measured for temperatures as low as 1.2 K with a resolution of 0.5 cm^{-1} .

B. Librational modes

1. Vibrational sidebands

Table I summarizes the peak vibrational frequencies of a number of different chalcogen hydride impurities in alkali halides measured at high resolution at 1.7 K. In addition, the observed peak frequencies of the librational sideband modes are tabulated; note that they lie near 300 cm^{-1} for all of these systems. These librational frequencies are quite large, implying that the orientational potential barriers must be high,¹³ on the order of 1000 cm^{-1} .

Figure 1 shows the vibrational sideband of $\text{KCl}:\text{SH}^-$ at three different temperatures, plotted in terms of the frequency shift relative to the strongest vibrational peak. The phonon sum band is evident between about 20 and 210 cm^{-1} and increases in strength with rising temperature. The librational sideband is clearly visible at +370 cm^{-1} at 1.7 K, but its strength disappears with increasing temperature. By 150 K there is little trace of it left.

Exactly the same behavior is seen for SD^- . Figure 2 compares the sidebands of SH^- and SD^- in KBr . The librational sideband of SD^- is shifted down in frequency relative to SH^- by roughly $\sqrt{2}$ (cf. Table I), confirming its assignment. Nevertheless, in both systems the strength of the libron vanishes by ~ 150 K.

The temperature dependences of the strength and width of the $\text{KBr}:\text{SD}^-$ librational sideband are plotted in Fig. 3. The area (filled circles) is seen to disappear by about 150 K. This

TABLE I. Fundamental vibrational peak frequencies, ω_{01} , deconvolved FWHM, γ_A , and fundamental librational-sideband peak frequencies, ω_{lib} , of the indicated systems at 1.7 K. The stretching modes were resolved by measuring crystals having impurity concentrations of no more than 100 ppm, while the sideband features were measured for crystals having up to 0.5 mol % XH^- concentrations.

System	ω_{01} (cm^{-1})	γ_A (cm^{-1})	ω_{lib} (cm^{-1})
$\text{KCl}:\text{}^{16}\text{OH}^-$	3642.11	0.11	298 ^a
$\text{KBr}:\text{}^{16}\text{OH}^-$	3617.47	0.12	310 ^a
$\text{RbCl}:\text{}^{16}\text{OH}^-$	3633.15	0.13	270
$\text{KCl}:\text{}^{16}\text{OD}^-$	2684.82	0.10	232 ^a
$\text{KCl}:\text{}^{32}\text{SH}^-$	2591.28	0.085	370
$\text{KBr}:\text{}^{32}\text{SH}^-$	2575.88	0.085	332
$\text{KI}:\text{}^{32}\text{SH}^-$	2558.94	0.028	289
$\text{RbCl}:\text{}^{32}\text{SH}^-$	2590.64	0.090	340 ^b
$\text{RbI}:\text{}^{32}\text{SH}^-$	2563.68	0.015	266
$\text{CsI}:\text{}^{32}\text{SH}^-$	2535.32	0.030	311
$\text{KBr}:\text{}^{32}\text{SD}^-$	1866.21	0.085	254
$\text{KCl}:\text{}^{80}\text{SeH}^-$	2322.9 ^c	0.085 ^c	371
$\text{KBr}:\text{}^{130}\text{TeH}^-$	2023.55 ^c	0.085 ^c	316

^aReference 2.

^bInterpolated from the lattice-constant dependence of the librational frequencies in other hosts.

^cReference 20.

anomalous temperature dependence of the strength is accompanied by an unusual variation of the librational linewidth (open circles). The observed broadening cannot be explained on the basis of elastic phonon scattering—a plot of Eq. (5.27) of Ref. 14 rises too steeply to fit the data. The linear rise in the linewidth with temperature above 25 K suggests that relaxation of the libron into two host phonons might be responsible instead. However, a plot of the lifetime-limited width due to such relaxation¹⁵ rises too slowly to fit the experimental results; a higher-order phonon decay process rises faster at low temperatures but bends over too sharply at high temperatures to explain the linear dependence. Thus, neither explanation works. Evidently, a model is needed which can simultaneously explain the thermal dependences of both the strength and the linewidth of the librational mode.

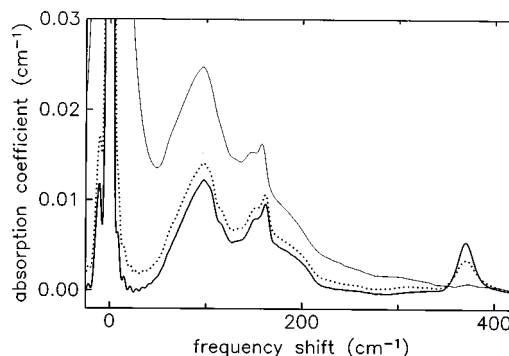


FIG. 1. Vibrational sideband spectra of nominally $\text{KCl}+0.4$ mol % KSH at 4 cm^{-1} resolution. The temperatures are 1.7 K (bold solid curve), 50 K (dotted curve), and 150 K (light solid curve).

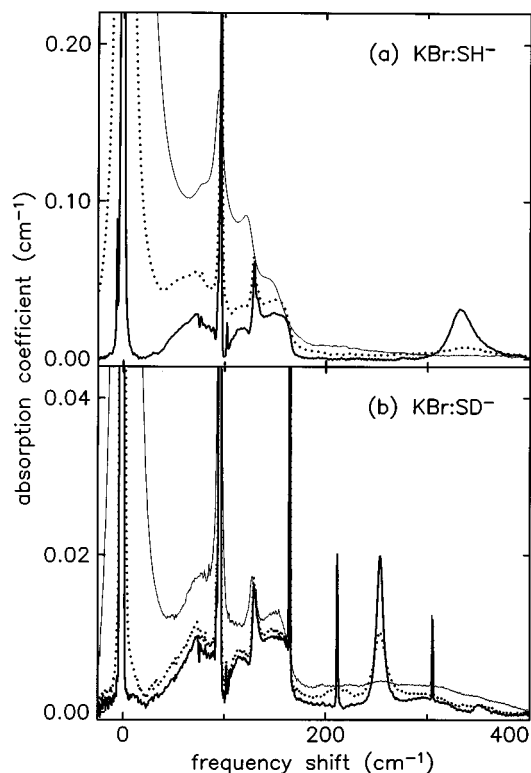


FIG. 2. Vibrational sideband spectra at 1 cm^{-1} resolution of nominally (a) KBr+0.5 mol % KSH at temperatures of 1.7 K (bold solid curve), 100 K (dotted curve), and 293 K (light solid curve); and (b) KBr+0.5 mol % KSD at temperatures of 1.7 K (bold solid curve), 50 K (dotted curve), and 150 K (light solid curve). The strong sharp line at $+95.6 \text{ cm}^{-1}$ in panel (a) is a KBr:SH $^-$ gap mode (Ref. 11); the analogous SD $^-$ gap mode in panel (b) almost exactly overlaps with the ω_3 vibrational mode of $^{11}\text{BO}_2^-$. The other sharp lines in panel (b) are due to foreign impurities: the ω_3 vibrational mode of $^{10}\text{BO}_2^-$ near $+165 \text{ cm}^{-1}$, the stretching mode of CN $^-$ near $+210 \text{ cm}^{-1}$, and the ω_3 vibrational mode of NCO $^-$ near $+305 \text{ cm}^{-1}$.

Figure 4 demonstrates that the SH $^-$ librational sideband vanishes in a similar manner in an unmixed KI crystal and in the same host when a small amount (2%) of a second alkali halide is mixed in. If the mixing ratio is made larger

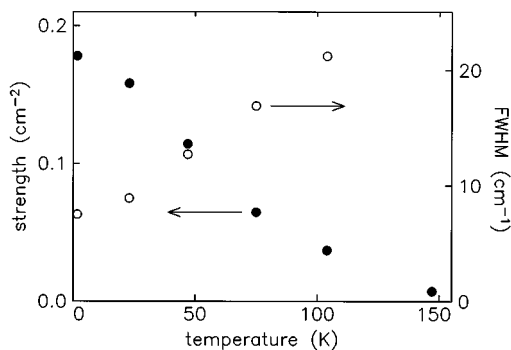


FIG. 3. Temperature dependences of the integrated strengths (filled circles) and of the deconvolved linewidths (open circles) of the background-subtracted librational sideband of nominally KBr + 0.5 mol % KSD.

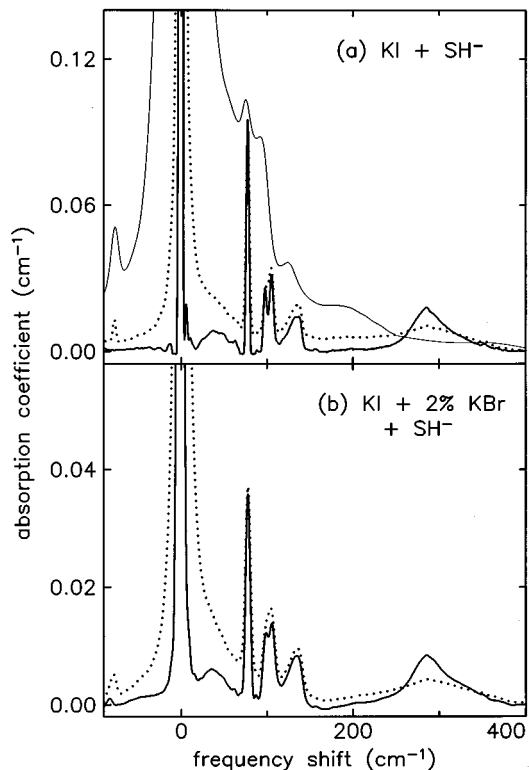


FIG. 4. Vibrational sideband spectra at 4 cm^{-1} resolution of nominally (a) KI+0.2 mol % KSH at temperatures of 1.7 K (bold solid curve), 50 K (dotted curve), and 293 K (light solid curve); (b) KI+2 mol % KBr+0.5 mol % KSH at temperatures of 1.7 K (bold solid curve) and 50 K (dotted curve). The sharp line in panel (a) at $+78 \text{ cm}^{-1}$ can be resolved into a gap mode doublet at $+77.0$ and $+78.3 \text{ cm}^{-1}$ at higher resolutions.

($\geq 10\%$), the phonon and libron sidebands become much less distinct. In panel (a) of Fig. 5, where the phonon and gap-mode sidebands still retain some sharpness, a librational sideband is visible which is only slightly broader than that of the corresponding unmixed systems and it is observed to disappear by $\sim 100 \text{ K}$. One might have expected the librational sidebands to broaden in these highly mixed crystals due to the variety of possible local environments of the SH $^-$ dipoles. But, for mixing ratios up to at least 10%, this does not appear to be the case. The broadest mode would be expected for the 50/50 host in panel (b), extending from at least the unmixed KBr:SH $^-$ librational frequency of 332 cm^{-1} to that of KCl:SH $^-$ at 370 cm^{-1} (cf. Table I). However, such a broadened sideband mode is not clearly visible in panel (b). It appears that the strength of the librational peak depends not only on temperature but also on the degree of local order in the crystal environment. In panel (c), a weak sideband peak appears to be present at low temperatures, but the poor signal-to-noise ratio combined with the reduced SH $^-$ concentration in the crystal (judging by the strength of the phonon sidebands) makes a definitive identification impossible.

Finally, Fig. 6 shows that the strength of the OH $^-$ libron in RbCl disappears with increasing temperature in exactly the same way as it does for SH $^-$ and SD $^-$, a phenomenon not reported by previous researchers.¹⁶ Similarly, the librational sidebands of SeH $^-$ and TeH $^-$ are observed to vanish, so that this temperature dependence of the librational mode

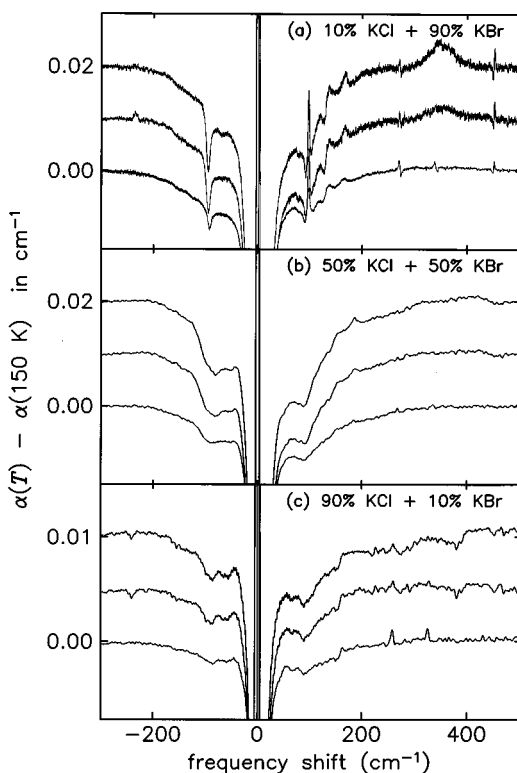


FIG. 5. Vibrational sideband spectra of nominally (a) 10 mol % KCl+90 mol % KBr+0.5 mol % KSH at 1 cm^{-1} resolution, (b) 50 mol % KCl+50 mol % KBr+0.5 mol % KSH at 4 cm^{-1} resolution, and (c) 90 mol % KCl+10 mol % KBr+0.5 mol % KSH at 4 cm^{-1} resolution. The temperatures from top to bottom in each panel are 1.7, 50, and 100 K and each curve has been displaced from the next by half a vertical unit, for clarity. Notice that the absorption is plotted relative to that at 150 K, by which temperature the libron should have vanished, in order to minimize background variations due to the extra long sample lengths. The librational sidebands would be expected to peak at frequencies approximately given by interpolating the peak frequencies of the unmixed crystals as given in Table I, namely at $+335$, $+350$, and $+365 \text{ cm}^{-1}$ for panels (a), (b), and (c), respectively. Notice that the SH^- gap mode of Fig. 2(a) is clearly visible (both in the sum and difference sidebands) for the crystal in panel (a), which has the largest KBr component of the three. Also notice that the spectral baseline is most irregular for the case of panel (c), for which the vertical axis has been expanded by a factor of 2, due to the low actual SH^- concentration in this crystal.

appears to be a universal feature of the diatomic chalcogen hydrides in sodium-chloride-structure alkali halides. (The case of the cesium-halide hosts is discussed later.)

A clearer picture of the librational modes and their temperature dependences can be obtained by subtracting off the background absorption in these figures (which is presumably determined mainly by two-phonon absorption) and expanding the axes appropriately. This has been done in Fig. 7 for a representative example of each of the four XH^- defects studied in this paper. Panel (a) presents the case of $\text{RbCl}:\text{OH}^-$. At 1.7 K, the librational mode is very well described as a Lorentzian with a width of 13 cm^{-1} and peaking at $+270 \text{ cm}^{-1}$, in excellent agreement with the results of Klein, Wedding, and Levine. Less satisfactory is the agreement at higher temperatures. We find that the linewidth increases only

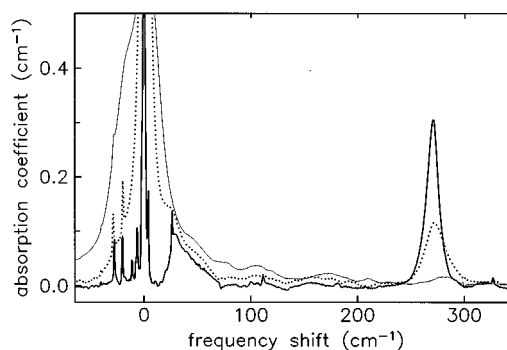


FIG. 6. Vibrational sideband spectra of nominally $\text{RbCl}+0.5 \text{ mol} \% \text{ RbOH}$ at 1 cm^{-1} resolution. The temperatures are 1.7 K (bold solid curve), 50 K (dotted curve), and 150 K (light solid curve). The peaks surrounding the vibrational mode have been briefly discussed in Ref. 1.

rather gradually with temperature, in a roughly linear manner, while the area under the peak rapidly disappears. In contrast, in Ref. 2 the librational sideband was reported to *double* in strength upon warming from 4 to 300 K, with a simultaneous ~ 13 -fold increase in its linewidth. On the other hand, the Raman spectra of OH^- in KCl and in KBr by Peascoe, Fenner, and Klein¹⁷ (for example, their Fig. 3) appear to essentially agree with our results; furthermore, these authors find that the A_{1g} component of the vibrational peak is narrowed relative to the IR peak with increasing temperature and interpret this as evidence that OH^- executes a rotational random walk at high temperatures with its angular motion damped by phonon collisions.^{18,19}

Figure 7(b) shows that the temperature dependence of the $\text{KCl}:\text{SH}^-$ librational sideband is very similar to that of $\text{RbCl}:\text{OH}^-$. Librational modes are also identified for SeH^- and TeH^- in the potassium halides, by running very long ($\sim 35 \text{ mm}$) samples, as is necessary because of the low dop-

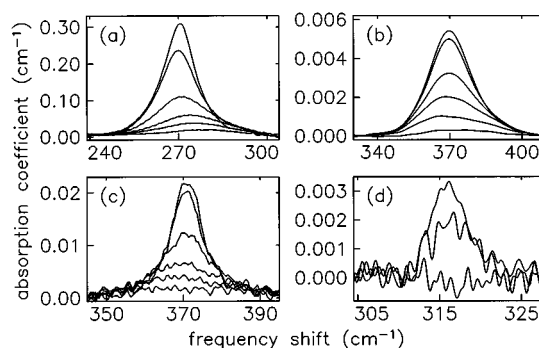


FIG. 7. Background-corrected librational-sideband absorption spectra of (a) $\text{RbCl}+\text{nominally } 0.5 \text{ mol} \% \text{ OH}^-$ with 1 cm^{-1} resolution—the temperatures, from top to bottom, are 1.7, 24, 53, 80, 112, and 150 K; (b) $\text{KCl}+\text{nominally } 0.4 \text{ mol} \% \text{ SH}^-$ at 4 cm^{-1} resolution—with temperatures of 1.7, 25, 50, 72, 101, and 152 K; (c) $\text{KCl}+0.023 \text{ mol} \% \text{ SeH}^-$ at 1 cm^{-1} resolution—the temperatures are 1.7, 25, 50, 75, 100, and 169 K; and (d) $\text{KBr}+0.0030 \text{ mol} \% \text{ TeH}^-$ at 0.5 cm^{-1} resolution—temperatures of 1.7, 75, and 200 K, from top to bottom. The horizontal axes give the frequency shifts relative to the dominant peak in the vibrational spectra at each temperature.

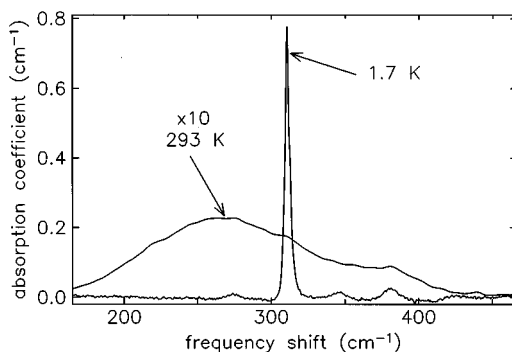


FIG. 8. Background-corrected absorption spectra of the librational sideband of nominally CsI+2 mol % RbI+0.05 mol % KSH at 1.7 K (1 cm^{-1} resolution) and 293 K (4 cm^{-1} resolution, with 10 times vertical expansion for clarity). The high-frequency bumps observable in both spectra, such as that at about +380 cm^{-1} , are background features believed to originate from trace amounts of oil on the interferometer, cryostat, and/or detector optics which vary slightly between the sample and reference runs. The horizontal axis specifies the frequency shift relative to the peak in the vibrational spectrum at each temperature.

ant concentrations.²⁰ Panels (c) and (d) show that the strengths are, again, temperature dependent. At 1.7 K, the linewidths are Lorentzian and rather narrow, 9 cm^{-1} for KCl:SeH⁻ and 5 cm^{-1} for KBr:TeH⁻. The signal-to-noise ratio is poor, owing to the low concentrations.

In contrast to the temperature-dependent strengths of the librational sidebands for the chalcogen hydrides in the sodium-chloride-structure alkali halides, Fig. 8 demonstrates that the librational sideband of CsI:SH⁻ remains visible, albeit greatly broadened and shifted in frequency, at RT. In fact, the area under the line is found to be equal at 1.7 and 293 K, to within 10%. Otto^{11,12} has discovered a number of other surprising spectroscopic properties of SH⁻ (and SeH⁻) in the cesium halides, including extremely strong phonon sidebands, librational overtones in the sideband spectra, strongly active direct librational modes (cf. Sec. II B 2), and in at least one case a vibrational overtone that is stronger than the fundamental. The hydroxide ion in the cesium halides has also been found²² to have a number of properties which distinguishes it from OH⁻ in the other alkali halides: the observation of high-temperature *P* and *R* branches thought to arise from translational motion of the defect from one off-center site to another, the occurrence of a variety of well-defined combination bands, and the thermally conserved strength of the $\sim 300 \text{ cm}^{-1}$ librational sideband. It thus appears that the potential surfaces describing the motions of the chalcogen hydrides in the cesium halides are fundamentally different from those in the sodium-chloride-structure hosts.

2. Direct lines

Further insight into the librational properties of the chalcogen hydrides can be obtained by studying the direct librational transitions in the far-infrared. Klein, Wedding, and Levine² have published a detailed study of the OH⁻ and OD⁻ direct librational modes in several sodium-chloride-structure alkali halides and compared them to the sideband

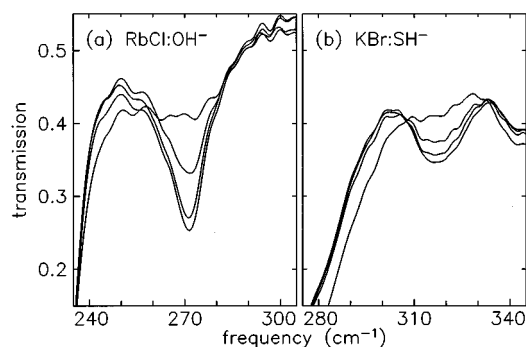


FIG. 9. Far-infrared transmission spectra at 1 cm^{-1} resolution of (a) a 1.25 mm sample of nominally RbCl+0.5 mol % RbOH, and (b) a 2.95 cm sample of nominally KBr+0.5 mol % KSH. The temperatures from bottom to top (for both samples) are 1.7, 10, 25, and 50 K. In absorbance at 1.7 K, the RbCl:OH⁻ (KBr:SH⁻) mode peaks at 271 (317) cm^{-1} , has a FWHM of 12 (15) cm^{-1} , and its amplitude is 5 (0.1) cm^{-1} . The sharp rise in the transmission in the low-frequency wings of the spectra in both panels is due to the host-phonon reststrahlen bands.

lines. Otto,¹¹ while not plotting the FIR spectra, has cited some useful information about the direct librational peaks of SH⁻, SD⁻, and SeH⁻ in the cesium halides. Interestingly enough, a substantial shift ($\sim 25 \text{ cm}^{-1}$) between the sideband and direct frequencies is found for the latter cases, in striking contrast to Klein's results where the shifts were minimal.

Attempts were made to look for the direct librational lines of SH⁻ in various potassium and rubidium halides at 1.7 K, but in general the expected far-infrared modes were not observed. One exception occurred for a very long ($\sim 3 \text{ cm}$), high-concentration (nominally 0.5 mol %) sample of KBr:SH⁻. The right-hand side of Fig. 9 shows a mode in this sample whose absorption strength is observed to vanish with increasing temperature. For comparison, the spectra of a thin sample of RbCl:OH⁻ is shown in the left-hand panel. At 1.7 K, the observed RbCl:OH⁻ line has a peak frequency of 271 cm^{-1} and a full width of half maximum (FWHM) in absorption of 12 cm^{-1} . These values agree to within 1 cm^{-1} with those of Fig. 7(a), confirming the identification of the mode as the libron. The FIR mode is ~ 15 times stronger than that of the sideband, as one might have roughly expected. Note especially that the strength of the direct peak is temperature dependent, just as was that of the sideband, an effect missed by previous investigators.²

The similarity of the FIR spectra of RbCl:OH⁻ and KBr:SH⁻ in Fig. 9 leads one to the natural conclusion that the observed mode in panel (b) is the direct librational line. In that case, however, there is a substantial frequency shift (although not as large as in the case of SH⁻ in the cesium halides¹¹) of the KBr:SH⁻ far-infrared mode compared to the corresponding sideband line (cf. Table I): the FIR peak is 15 cm^{-1} lower in frequency. Furthermore, the ratio of FIR-to-sideband strengths for KBr:SH⁻ is merely ~ 3 , implying that the direct SH⁻ libron is only rather weakly dipole allowed. Finally, the OH⁻ sidebands are about an order of magnitude stronger, on average, than those of SH⁻ at the same dopant concentrations. The origin of these differences for the librational modes of OH⁻ and SH⁻ are not presently clear.

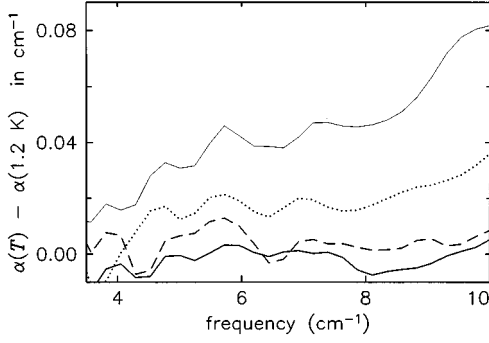


FIG. 10. Very-far-infrared absorption spectra relative to 1.2 K of a sample of nominally KBr+0.5 mol % KSH at temperatures of 27 K (bold solid curve), 34 K (dashed curve), 54 K (dotted curve), and 84 K (light solid curve) at 0.5 cm^{-1} resolution.

C. Diffusional modes

Absorption measurements in the millimeter-wave frequency range were performed on a couple of different SH^- samples, in an effort to locate the absorption strength lost by the librational mode. Figure 10 presents the results at four different temperatures for a sample of nominally KBr +0.5 mol % SH^- . A Debye-like spectrum which grows in strength with increasing temperature is evident. This temperature-dependent spectrum is not seen in an otherwise-identical undoped piece of KBr. At the two highest temperatures, a knee in the data is observed at $\sim 9 \text{ cm}^{-1}$ due to the onset of two-phonon-difference absorption, analogous to what has been seen previously²³ in pure KI and NaCl.

It appears that with rising temperature the librational absorption strength associated with the impurity is increasingly replaced by a Debye-like spectrum at low frequencies. This Debye spectrum is not apparent in the vibrational sideband region of Fig. 2(a) since it is buried within the broad high-temperature vibrational peaks.

III. THEORETICAL ANALYSIS

Figure 11 shows the thermally induced loss of the librational sideband absorption strength (normalized to the low-

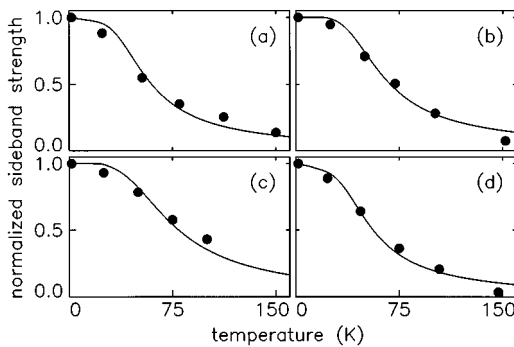


FIG. 11. Temperature dependences of the librational sideband strengths, normalized to the 1.7 K values, for (a) RbCl:OH⁻, (b) KCl:SH⁻, (c) KCl:SeH⁻, and (d) KBr:SD⁻. The filled circles are obtained by integrating the areas under the background-corrected sidebands. The continuous curves are fits to the generalized jump-rotational-diffusion model, using the parameters given in Table II.

temperature value) for four different chalcogen hydrides in three different hosts. The filled circles give the experimental values, obtained by integrating the background-subtracted peaks such as those plotted in Fig. 7. It is evident that the shapes of the curves are similar for all of these systems.

In order to account for these data, we propose that there are two elastic configurations for this molecular defect with very different ground-state energies: in one configuration (at low temperatures) the molecule is orientationally confined but can librate and also tunnel between the librational wells, while in the other configuration (at higher temperatures) the molecule undergoes rotationally diffusive motion. In a brief report, we have previously outlined a model with one angular degree of freedom which can account for this unusual temperature dependence of the strength by having the molecule jump between these two elastic configurations with temperature-dependent dwell times.¹² Here, we generalize this model by including both angular degrees of freedom, θ and ϕ , of a diatomic impurity in a crystal and provide a more complete description of the dynamics associated with this process. The possibility of tunneling shall be ignored in the classical model presented here.

The motion of any given dipole is modeled as a stochastic process which is subdivided into successive time steps $0, 1, 2, \dots$. Suppose that the dipole is initially oriented at $\Omega_0 \equiv (\theta_0, \phi_0)$ at time $t=0$ and librates for an average time τ_A ; next, in time step 1, the dipole jumps to the rotationally diffusive state in which it remains for an average time τ_B ; in step 2, it is librating again; and so forth. The self-correlation function, G_s , which is the probability of finding the dipole with orientation Ω at time t , can be written as a sum over each step j :

$$G_s(\Omega_0; \Omega, t) = \sum_{j=0}^{\infty} F_j(\Omega_0; \Omega, t), \quad (1)$$

where

$$F_0(\Omega_0; \Omega, t) = p_A(t) g_A(\Omega_0; \Omega, t), \quad (2a)$$

$$F_1(\Omega_0; \Omega, t) = - \int_0^t dt_1 \int d\Omega_1 p_B(t-t_1) g_B(\Omega_1; \Omega, t-t_1) \\ \times \dot{p}_A(t_1) g_A(\Omega_0; \Omega_1, t_1), \quad (2b)$$

$$F_2(\Omega_0; \Omega, t) = (-1)^2 \int_0^t dt_2 \int_0^{t_2} dt_1 \int d\Omega_1 \int d\Omega_2 \\ \times p_A(t-t_2) g_A(\Omega_2; \Omega, t-t_2) \dot{p}_B(t_2-t_1) \\ \times g_B(\Omega_1; \Omega_2, t_2-t_1) \dot{p}_A(t_1) g_A(\Omega_0; \Omega_1, t_1), \quad (2c)$$

and so on. The functions $g_i(\Omega_0; \Omega, t)$, where $i=A$ or B , describe how the reorienting dipoles in the librational (A) and rotationally diffusive (B) states, respectively, spread out from each other and $p_i \equiv \exp(-t/\tau_i)$ are the corresponding probabilities that any given dipole remains in these states. For a substitutional diatomic in a cubic crystal, as is the case in this paper, $g_i(\Omega_0; \Omega, t)$ depends on Ω and Ω_0 only through their difference, $\Omega - \Omega_0$. Hence they can be expanded in terms of the spherical harmonics Y_{lm} as

$$g_A(\Omega_0; \Omega, t) = \sum_{l,m} a_l(t) Y_{lm}(\Omega) Y_{lm}^*(\Omega_0) \quad (3a)$$

and

$$g_B(\Omega_0; \Omega, t) = \sum_{l,m} b_l(t) Y_{lm}(\Omega) Y_{lm}^*(\Omega_0), \quad (3b)$$

with expansion coefficients $a_l(t)$ and $b_l(t)$.

In order to obtain the IR absorption coefficient, one needs an expression for the complex polarizability of an impurity dipole, $\hat{\alpha}(\omega)$. This can be obtained from the Kubo relation,²⁴

$$\hat{\alpha}(\omega) \equiv \alpha_1(\omega) - i\alpha_2(\omega) = \frac{\mu^2}{3kT} \left[1 - i\omega \int_0^\infty dt e^{-i\omega t} C(t) \right], \quad (4)$$

where μ is the permanent dipole moment of the rotor and $C(t)$ is the dipole-dipole autocorrelation function, which is related to Eq. (1) by

$$C(t) \equiv \langle \mathbf{n}(t) \cdot \mathbf{n}(0) \rangle = \int d\Omega P_1(\Omega \cdot \Omega_0) G_s(\Omega_0; \Omega, t). \quad (5)$$

Here $\mathbf{n}(t)$ is the unit vector along the dipole moment at time t and P_1 is the first-order Legendre polynomial whose argument is $\Omega \cdot \Omega_0 = \cos\theta \cos\theta_0 + \sin\theta \sin\theta_0 \cos(\phi - \phi_0)$. In order to obtain the Fourier transform of $C(t)$, we first evaluate the Fourier transform of $G_s(\Omega_0; \Omega, t)$ by substituting the functions F_j to obtain

$$\begin{aligned} & \int_0^\infty dt e^{-i\omega t} G_s(\Omega_0; \Omega, t) \\ &= \sum_{l,m} Y_{lm}(\Omega) \frac{A_l(\omega) + A_l(\omega)B_l(\omega)/\tau_A}{1 - A_l(\omega)B_l(\omega)/(\tau_A\tau_B)} Y_{lm}^*(\Omega_0) \\ &= \sum_l \frac{A_l(\omega) + A_l(\omega)B_l(\omega)/\tau_A}{1 - A_l(\omega)B_l(\omega)/(\tau_A\tau_B)} \frac{2l+1}{4\pi} P_l(\Omega \cdot \Omega_0), \end{aligned} \quad (6)$$

where

$$A_l(\omega) = \int_0^\infty dt e^{-i\omega t} p_A(t) a_l(t), \quad (7a)$$

and

$$B_l(\omega) = \int_0^\infty dt e^{-i\omega t} p_B(t) b_l(t). \quad (7b)$$

By inserting Eq. (6) into Eq. (5) and making use of the orthogonality of the Legendre polynomials, one finds that

$$\int_0^\infty dt e^{-i\omega t} C(t) = \frac{A_1(\omega) + A_1(\omega)B_1(\omega)/\tau_A}{1 - A_1(\omega)B_1(\omega)/(\tau_A\tau_B)}. \quad (8)$$

Therefore, the IR spectrum probes only the $l=1$ component of $G_s(\Omega_0; \Omega, t)$. Here we have assumed that the dipole is initially in the librational state. In general, however, the dipole can start in either the librational or rotationally diffusive state, so that $G_s(\Omega_0; \Omega, t)$ must be averaged over both Eq. (8) and the analogous rotationally diffusive expression with

the respective weight factors $\tau_A/(\tau_A + \tau_B)$ and $\tau_B/(\tau_A + \tau_B)$. Thus, one obtains for the complex polarizability

$$\begin{aligned} \hat{\alpha}(\omega) = \frac{\mu^2}{3kT} & \left\{ 1 - i\omega \left[\frac{\tau_A}{\tau_A + \tau_B} \frac{A_1(\omega) + A_1(\omega)B_1(\omega)/\tau_A}{1 - A_1(\omega)B_1(\omega)/(\tau_A\tau_B)} \right. \right. \\ & \left. \left. + \frac{\tau_B}{\tau_A + \tau_B} \frac{B_1(\omega) + A_1(\omega)B_1(\omega)/\tau_B}{1 - A_1(\omega)B_1(\omega)/(\tau_A\tau_B)} \right] \right\}. \end{aligned} \quad (9)$$

Consider Eq. (9) in the limits of very low or high temperatures. At low temperatures the dipole is trapped in the librational potential well ($\tau_A \rightarrow \infty$) producing an IR absorption line at the librational frequency, while at high temperatures it spends an increasing amount of time in the rotationally diffusive configuration so that oscillator strength is transferred from the librational mode to a Debye relaxational spectrum. This transfer is controlled by the temperature dependences of the lifetimes τ_A and τ_B , which depend in turn on the relative energy separation of the two elastic configurations. If this energy separation is much smaller for the sodium-chloride than the cesium-chloride structure alkali halides, Eq. (9) would account in a natural way for the way different temperature dependences of the observed librational strengths.

In order to apply this model in detail to the experimental data for XH^- , we need expressions for $A_1(\omega)$ and $B_1(\omega)$. For this purpose, we treat the librorator as a simple Lorentz oscillator and use a generalized-Debye model for the rotationally diffusive configuration. One can see from Eqs. (7a) and (7b) that the effect of a finite dwell time τ_i ($i=A, B$) is to shift the frequency by an amount $-i/\tau_i$. Evaluating Eq. (9) in the limit $\tau_A \rightarrow \infty$ yields

$$A_1(\omega) = \frac{1}{i\tilde{\omega}_A} \left[1 - \frac{kT/I}{\omega_{\text{lib}}^2 - \tilde{\omega}_A^2 + i\gamma_A\tilde{\omega}_A} \right], \quad (10)$$

where I is the moment of inertia of the dipole, ω_{lib} is its librational frequency, γ_A is the spectral FWHM of the librational peak, and $\tilde{\omega}_A \equiv \omega - i/\tau_A$. Evaluating Eq. (9) for $\tau_B \rightarrow \infty$, on the other hand, specifies the rotationally diffusive configuration. Since Debye's original one-pole formula does not conserve oscillator strength, we instead use a two-pole expression which does.²⁴ The result is

$$B_1(\omega) = \frac{1}{i\tilde{\omega}_B} [1 - (1 + i\tilde{\omega}_B\tau_D)^{-1} (1 + i\tilde{\omega}_B/\gamma_B)^{-1}], \quad (11)$$

where $\tilde{\omega}_B \equiv \omega - i/\tau_B$, γ_B is the damping constant, and $\tau_D \equiv I\gamma_B(kT)^{-1}$ is the Debye relaxation time.

Experimentally, while the strengths of the librational modes disappear with increasing temperature, their center frequencies do not shift significantly (cf. Fig. 7), indicating that the librational potential wells are not thermally softened. Clearly, the barrier heights of these wells must be much greater than 150 K, the temperature by which the librational absorption strengths have vanished. On the other hand, this disappearance suggests that the rotationally diffusive configuration lies ~ 150 K higher in energy than the librational one. We therefore speculate that the elastic potential associated with this defect-lattice system has a deep, narrow energy minimum (A) and a much broader and shallower energy minimum (B) schematically like that sketched in Fig. 2 of

TABLE II. Model parameters for the two elastic configurations of the alkali-halide-doped diatomic-chalcogen-hydride systems plotted in Fig. 11: ω_A is the Debye frequency of the host; ω_B is the attempt frequency in the rotationally diffusive configuration; and T_A and T_B specify the potential barrier heights.

System	ω_A (cm ⁻¹)	ω_B (cm ⁻¹)	T_A (K)	T_B (K)
RbCl:OH ⁻	115	7.2	780	600
KCl:SH ⁻	161	10.1	900	700
KCl:SeH ⁻	161	13.4	925	700
KBr:SD ⁻	120	7.5	800	625

Ref. 12. Elastic configuration *A* supports high-frequency librational motion of the molecule, while configuration *B* favors nearly-free rotations about the lattice site. The relevant barrier heights are identified in the figure.

The temperature dependences of the times spent in each configuration are assumed to be given by²⁵

$$1/\tau_A = \omega_A \exp(-T_A/T) \quad (12a)$$

and

$$1/\tau_B = \omega_B \exp(-T_B/T), \quad (12b)$$

where ω_A and ω_B are characteristic attempt frequencies of the defect system in its librational and rotationally diffusive configurations, respectively. The attempt frequency in the librational configuration is taken to be the Debye frequency of the host; ω_B and the barrier heights, kT_A and kT_B , are free parameters of the model. Fitted values for the four systems in Fig. 11 are listed in Table II. Owing to the lack of detailed experimental data in the millimeter-wave frequency region, we assume that $\gamma_B = \gamma_A$, where γ_A is obtained by fitting the experimental linewidths of the librational modes as a function of temperature.

With these parameters, the temperature-dependent absorption spectra, which are proportional to $\omega\alpha_2(\omega)$, can be calculated. With increasing temperature, oscillator strength is transferred from the librational modes to the low-frequency Debye spectra. While the librational absorption peaks broaden and vanish with increasing temperature, their center frequencies remain essentially unchanged, reproducing the experimental data. The theoretical strengths of the librational modes at each temperature can be found by integration and are plotted as the solid curves in Fig. 11(a)–11(d). The results agree with the experimental values (filled circles) to within the experimental uncertainties.

IV. CONCLUSIONS

A ~ 300 cm⁻¹ librational sideband is identified for SH⁻, SeH⁻, and TeH⁻ in the fcc hosts, analogous to a correspond-

ing mode previously discovered for OH⁻ in the alkali halides² and for SH⁻ and SeH⁻ in the cesium halides.¹¹ The SH⁻ sideband shifts down in frequency by approximately $\sqrt{2}$ upon deuteration, confirming the assignment. The large frequencies of the XH⁻ librons suggest that their orientational potential barriers must be on the order of 1000 cm⁻¹, which have traditionally been modeled by the standard Devonshire potential. Unexplained by this model, however, is the disappearance of the librational-sideband absorption strengths by ~ 150 K, at temperatures far lower than expected on the basis of thermal saturation of the librational-level populations.⁶ A similar temperature dependence is observed for all of the chalcogen hydrides in the sodium-chloride-structure hosts, both for the vibrational sidebands and for the direct FIR librational transitions. There is some evidence which suggests that the absorption strength of the librational sideband of AgCl:OH⁻ similarly disappears above liquid-nitrogen temperatures.²⁶ Given that AgCl has a sodium-chloride structure, it appears that the above model may be applicable to this system as well. However, covalency effects play a significant role in the silver halides as contrasted with the alkali halides.²⁷ Thus, a more detailed investigation of the diatomic hydrides in the silver salts may shed additional light on the rich orientational dynamics of these model systems. On the other hand, the strength of the librational mode is conserved for CsI:SH⁻, as well as for OH⁻ in the cesium halides,²² suggesting that the host crystal structure plays a determining role in the temperature-dependent dynamics.

The thermally activated loss of the librational strength of the diatomic hydrides in fcc salt crystals has been explained by introducing two elastic configurations of the defect-lattice system: a low-energy one which supports its own defect-induced absorption spectrum including librational motion of the impurity molecule, and a higher-energy configuration which supports nearly-free diffusional rotation of the molecular moment. The observed spectra are successfully described by a generalized jump-rotational-diffusion model, wherein the librations of the diatomics are interrupted by hops from one elastic configuration to another. The lattice dynamics which produce multiple elastic configurations for such simple lattice-defect systems remain a mystery.

ACKNOWLEDGMENTS

We thank M. V. Klein, R. O. Pohl, and C. R. Pollock for the OH⁻ and OD⁻ samples used in this study. Sample-growing efforts by S. Baek and S. Wielandy are also gratefully acknowledged. J. Tu is to be thanked for retrieval of archival data. Discussions with U. Happek have been helpful. This work is supported by NSF-DMR-9312381, NASA-NAGW-2768, and ARO-DAAL03-92-G-0369. Use was made of the MRL Facilities supported by DMR-9121654.

*Present address: Dept. of Physics, University of West Florida, Pensacola, FL 32514–5751.

¹B. Wedding and M. V. Klein, Phys. Rev. **177**, 1274 (1969).

²M. V. Klein, B. Wedding, and M. A. Levine, Phys. Rev. **180**, 902 (1969).

³C.-K. Chi and E. R. Nixon, J. Phys. Chem. Solids **33**, 2101 (1972).

⁴J. Otto, Phys. Status Solidi B **151**, 363 (1989).

⁵C. E. Mungan, U. Happek, J. T. McWhirter, and A. J. Sievers, in *Defects in Insulating Materials*, edited by O. Kanert and J.-M. Spaeth (World Scientific, Singapore, 1993), Vol. 1, p. 536.

⁶C. E. Mungan, U. Happek, and A. J. Sievers, J. Lumin. **58**, 33 (1994).

⁷F. Lüty, Cryst. Latt. Defects Amorph. Mater. **12**, 343 (1985).

- ⁸W. D. Seward and V. Narayanamurti, *Phys. Rev.* **148**, 463 (1966).
- ⁹C. E. Mungan, R. C. Spitzer, J. P. Sethna, and A. J. Sievers, *Phys. Rev. B* **43**, 43 (1991).
- ¹⁰C. K. Chau, M. V. Klein, and B. Wedding, *Phys. Rev. Lett.* **17**, 521 (1966).
- ¹¹J. Otto, *Phys. Status Solidi B* **142**, 105 (1987).
- ¹²R. Lai, C. E. Mungan, and A. J. Sievers, *Phys. Rev. Lett.* **76**, 1864 (1996).
- ¹³M. Indere and K.-L. Jüngst, *J. Phys. Chem. Solids* **37**, 1105 (1976).
- ¹⁴A. S. Barker, Jr. and A. J. Sievers, *Rev. Mod. Phys.* **47**, S1 (1975).
- ¹⁵A. Nitzan, S. Mukamel, and J. Jortner, *J. Chem. Phys.* **60**, 3929 (1974).
- ¹⁶At the end of Sec. III of Ref. 2, some remarks are made about the temperature dependence of the librational strength. We suggest, based on careful examination of their spectra in Ref. 1, that the apparent contradiction with our data is due to an uncorrected overall baseline shift in their measurements.
- ¹⁷J. G. Peascoe, W. R. Fenner, and M. V. Klein, *J. Chem. Phys.* **60**, 4208 (1974).
- ¹⁸W. R. Fenner and M. V. Klein, in *Light Scattering Spectra of Solids*, edited by G. B. Wright (Springer-Verlag, New York, 1969), p. 497.
- ¹⁹J. G. Peascoe and M. V. Klein, *J. Chem. Phys.* **59**, 2394 (1973).
- ²⁰C. E. Mungan, U. Happek, T. Z. Hossain, and A. J. Sievers, *J. Phys. Chem. Solids* **56**, 735 (1995).
- ²¹J. Otto, *Phys. Status Solidi B* **148**, 489 (1988).
- ²²M. Krantz and F. Lüty, *Phys. Rev. B* **37**, 7038 (1988).
- ²³S. P. Love, W. P. Ambrose, and A. J. Sievers, *Phys. Rev. B* **39**, 10 352 (1989).
- ²⁴B. K. P. Scaife, *Principles of Dielectrics* (Clarendon, Oxford, 1989), p. 350.
- ²⁵H. Fröhlich, *Theory of Dielectrics*, 2nd ed. (Clarendon, Oxford, 1958), p. 68.
- ²⁶F. J. Sterk and R. C. Hanson, *Solid State Commun.* **9**, 1473 (1971).
- ²⁷W. von der Osten, in *Semiconductors: Physics of II-VI and I-VII Compounds, Semimagnetic Semiconductors*, edited by O. Madelung, Landolt-Börnstein, New Series, Vol. III/7b (Springer-Verlag, Berlin, 1982), p. 253.